CLEO CONF 97-01
EPS 97-339

Exclusive Reconstruction of $B \to D^{(*)}(n\pi)^-$ Decays

CLEO Collaboration

(July 25, 1997)

Abstract

Hadronic two-body B decay modes are reconstructed exclusively using 3.1 fb^{-1} of data at the $\Upsilon(4S)$ collected with CLEO II detector. Two classes of decay modes are discussed: $B^0 \to D^{(*)+}(n\pi)^-$ and $B^- \to D^{(*)0}(n\pi)^-$. Branching fraction results are then used to determine the magnitude and relative sign of the BSW parameters $|a_1|$ and a_2/a_1.

B. Barish,[1] M. Chadha,[1] S. Chan,[1] G. Eigen,[1] J. S. Miller,[1] C. O'Grady,[1] M. Schmidtler,[1] J. Urheim,[1] A. J. Weinstein,[1] F. Würthwein,[1] D. W. Bliss,[2] G. Masek,[2] H. P. Paar,[2] S. Prell,[2] M. Sivertz,[2] V. Sharma,[2] D. M. Asner,[3] J. Gronberg,[3] T. S. Hill,[3] D. J. Lange,[3] S. Menary,[3] R. J. Morrison,[3] H. N. Nelson,[3] T. K. Nelson,[3] C. Qiao,[3] J. D. Richman,[3] D. Roberts,[3] A. Ryd,[3] M. S. Witherell,[3] R. Balest,[4] B. H. Behrens,[4] W. T. Ford,[4] H. Park,[4] J. Roy,[4] J. G. Smith,[4] J. P. Alexander,[5] C. Bebek,[5] B. E. Berger,[5] K. Berkelman,[5] K. Bloom,[5] D. G. Cassel,[5] H. A. Cho,[5] D. S. Crowcroft,[5] M. Dickson,[5] P. S. Drell,[5] K. M. Ecklund,[5] R. Ehrlich,[5] A. D. Foland,[5] P. Gaidarev,[5] R. S. Galik,[5] L. Gibbons,[5] B. Gittelman,[5] S. W. Gray,[5] D. L. Hartill,[5] B. K. Heltsley,[5] P. I. Hopman,[5] J. Kandaswamy,[5] P. C. Kim,[5] D. L. Kreinick,[5] T. Lee,[5] Y. Liu,[5] G. S. Ludwig,[5] N. B. Mistry,[5] C. R. Ng,[5] E. Nordberg,[5] M. Ogg,[5,*] J. R. Patterson,[5] D. Peterson,[5] D. Riley,[5] A. Soffer,[5] B. Valant-Spaight,[5] C. Ward,[5] M. Athanas,[6] P. Avery,[6] C. D. Jones,[6] M. Lohner,[6] C. Prescott,[6] J. Yelton,[6] J. Zheng,[6] G. Brandenburg,[7] R. A. Briere,[7] A. Ershov,[7] Y. S. Gao,[7] D. Y.-J. Kim,[7] R. Wilson,[7] H. Yamamoto,[7] T. E. Browder,[8] Y. Li,[8] J. L. Rodriguez,[8] T. Bergfeld,[9] B. I. Eisenstein,[9] J. Ernst,[9] G. E. Gladding,[9] G. D. Gollin,[9] R. M. Hans,[9] E. Johnson,[9] I. Karliner,[9] M. A. Marsh,[9] M. Palmer,[9] M. Selen,[9] J. J. Thaler,[9] K. W. Edwards,[10] A. Bellerive,[11] R. Janicek,[11] D. B. MacFarlane,[11] P. M. Patel,[11] A. J. Sadoff,[12] R. Ammar,[13] P. Baringer,[13] A. Bean,[13] D. Besson,[13] D. Coppage,[13] C. Darling,[13] R. Davis,[13] N. Hancock,[13] S. Kotov,[13] I. Kravchenko,[13] N. Kwak,[13] S. Anderson,[14] Y. Kubota,[14] S. J. Lee,[14] J. J. O'Neill,[14] S. Patton,[14] R. Poling,[14] T. Riehle,[14] V. Savinov,[14] A. Smith,[14] M. S. Alam,[15] S. B. Athar,[15] Z. Ling,[15] A. H. Mahmood,[15] H. Severini,[15] S. Timm,[15] F. Wappler,[15] A. Anastassov,[16] J. E. Duboscq,[16] D. Fujino,[16,†] K. K. Gan,[16] T. Hart,[16] K. Honscheid,[16] H. Kagan,[16] R. Kass,[16] J. Lee,[16] M. B. Spencer,[16] M. Sung,[16] A. Undrus,[16,‡] R. Wanke,[16] A. Wolf,[16] M. M. Zoeller,[16] B. Nemati,[17] S. J. Richichi,[17] W. R. Ross,[17] P. Skubic,[17] M. Bishai,[18] J. Fast,[18] J. W. Hinson,[18] N. Menon,[18] D. H. Miller,[18] E. I. Shibata,[18] I. P. J. Shipsey,[18] M. Yurko,[18] S. Glenn,[19] S. D. Johnson,[19] Y. Kwon,[19,§] S. Roberts,[19] E. H. Thorndike,[19] C. P. Jessop,[20] K. Lingel,[20] H. Marsiske,[20] M. L. Perl,[20] D. Ugolini,[20] R. Wang,[20] X. Zhou,[20] T. E. Coan,[21] V. Fadeyev,[21] I. Korolkov,[21] Y. Maravin,[21] I. Narsky,[21] V. Shelkov,[21] J. Staeck,[21] R. Stroynowski,[21] I. Volobouev,[21] J. Ye,[21] M. Artuso,[22] A. Efimov,[22] M. Goldberg,[22] D. He,[22] S. Kopp,[22] G. C. Moneti,[22] R. Mountain,[22] S. Schuh,[22] T. Skwarnicki,[22] S. Stone,[22] G. Viehhauser,[22] X. Xing,[22] J. Bartelt,[23] S. E. Csorna,[23] V. Jain,[23,**] K. W. McLean,[23] S. Marka,[23] R. Godang,[24] K. Kinoshita,[24] I. C. Lai,[24] P. Pomianowski,[24] S. Schrenk,[24] G. Bonvicini,[25] D. Cinabro,[25] R. Greene,[25]

*Permanent address: University of Texas, Austin TX 78712

†Permanent address: Lawrence Livermore National Laboratory, Livermore, CA 94551.

‡Permanent address: BINP, RU-630090 Novosibirsk, Russia.

§Permanent address: Yonsei University, Seoul 120-749, Korea.

**Permanent address: Brookhaven National Laboratory, Upton, NY 11973.

L. P. Perera,[25] and G. J. Zhou[25]

[1]California Institute of Technology, Pasadena, California 91125
[2]University of California, San Diego, La Jolla, California 92093
[3]University of California, Santa Barbara, California 93106
[4]University of Colorado, Boulder, Colorado 80309-0390
[5]Cornell University, Ithaca, New York 14853
[6]University of Florida, Gainesville, Florida 32611
[7]Harvard University, Cambridge, Massachusetts 02138
[8]University of Hawaii at Manoa, Honolulu, Hawaii 96822
[9]University of Illinois, Champaign-Urbana, Illinois 61801
[10]Carleton University, Ottawa, Ontario, Canada K1S 5B6
and the Institute of Particle Physics, Canada
[11]McGill University, Montréal, Québec, Canada H3A 2T8
and the Institute of Particle Physics, Canada
[12]Ithaca College, Ithaca, New York 14850
[13]University of Kansas, Lawrence, Kansas 66045
[14]University of Minnesota, Minneapolis, Minnesota 55455
[15]State University of New York at Albany, Albany, New York 12222
[16]Ohio State University, Columbus, Ohio 43210
[17]University of Oklahoma, Norman, Oklahoma 73019
[18]Purdue University, West Lafayette, Indiana 47907
[19]University of Rochester, Rochester, New York 14627
[20]Stanford Linear Accelerator Center, Stanford University, Stanford, California 94309
[21]Southern Methodist University, Dallas, Texas 75275
[22]Syracuse University, Syracuse, New York 13244
[23]Vanderbilt University, Nashville, Tennessee 37235
[24]Virginia Polytechnic Institute and State University, Blacksburg, Virginia 24061
[25]Wayne State University, Detroit, Michigan 48202

I. INTRODUCTION

Studies of the two body decays of the B meson provide important information on both weak and hadronic interactions of heavy flavored mesons. In particular, tests of the factorization hypothesis and theoretical model predictions can be performed using precise measurements of the properties of these decays [1–5]. In this analysis we present new results on twelve two-body hadronic decays of the B^0 and B^- mesons using the entire CLEO II data set. The modes investigated consist of a combinations of a 1, 2 or 3 pion resonance with a vector or pseudoscalar charmed meson.

II. DATA SAMPLE AND GLOBAL EVENT SELECTION

This analysis uses the 3.1 fb^{-1} taken at the $\Upsilon(4S)$ with the CLEO II detector [6]. In addition, 1.4 fb^{-1} of data taken 26 MeV below the $\Upsilon(4S)$ were used to model the continuum background; the dominate source of background in the analysis. The on-4S sample corresponds to 3.3 million $B\bar{B}$ pairs and is approximately three times as large as the sample used in the previous CLEO II version of this analysis [7,8].

Events were selected from a hadronic sub-sample of the complete CLEO II dataset. The sub-sample includes events that have passed the following requirements: the total event energy deposited in the calorimeter is less than 65% but greater than 20% of the center-of-mass energy and the number of charged tracks is greater than or equal to four. To reduce contamination from continuum background we rejected events with ratios of 1^{st} to 2^{nd} Fox-Wolfram [9] moments less than 0.5.

III. CANDIDATE SELECTION CRITERIA

A. Charged tracks

All charged tracks were required to pass loose particle ID and impact parameter cuts. Charged tracks were also required to have an impact parameter consistent with tracks originating at the beam spot. The selection criteria are functions of both momentum and azimuthal angle and take into account the shape of the beam-spot and effects from multiple scattering. For particle ID, we require that tracks have a sufficient number of hits in the drift chamber to allow for good particle ID and require 3σ (σ is a standard deviation) K/π consistency from energy loss in the drift chamber. For tracks used as slow pion candidates, when forming D^{*+}, we relax the impact parameter cut and remove all particle ID requirements.

B. Light mesons, π^0, ρ and a_1

Candidate π^0s were selected from two photon combinations with a reconstructed mass required to be within 2.5σ of the π^0 measured in an inclusive data sample. The measured widths are assymeteric, and both the mean mass and the widths vary as a function of π^0 momenta. Candidates with momenta less than 250 MeV were rejected if one of the photons

fell within the endcap or endcap-barrel overlap region of the detector. All candidates were kinematically fit with their masses constrained to the known π^0 mass. A χ^2 cut of 9.0 was imposed. Candidate ρ mesons were selected from $\pi\pi$ combinations with an invariant mass within $\pm$150MeV of the nominal ρ mass. The mass of the a_1^- candidates was required to fall between 1.0 GeV and 1.6 GeV. Only the $\rho^0\pi^-$ mode was used to form the a_1 candidates[1]. Since there are two possible combinations of the 3 pions that can form a $\rho^0\pi^-$ both were examined and if at least one of the combination was within 150 MeV of the nominal ρ^0 mass the combination was accepted as an a_1 candidate.

C. Charmed particles

Three decay modes, $K^-\pi^+$, $K^-\pi^+\pi^0$ and the $K^-\pi^+\pi^-\pi^+$, were used to form D^0 candidates. Only the $K^+\pi^-\pi^-$ mode was used to form D^+ candidates. These are the cleanest modes with relatively large efficiency$\times D$ branching fraction. A $2.5\sigma_{m_D}$ mass requirement was imposed on all D^0 and D^+ candidates.

For D^* candidates we required the mass difference between the D^0 and the D^* to be within 2.5σ of the nominal D^* – D^0 mass difference. As with the pseudoscalar decays, we only considered charmed vector meson decay modes with both large branching fractions and low backgrounds. Thus only two decay modes: the $D^{*+} \to D^0\pi^+$ and $D^{*0} \to D^0\pi^0$ mode were used.

IV. B MESON CANDIDATES

To calculate the branching fraction we need to determine the number of fully reconstructed B mesons in our sample. To do so we used the beam constrained mass ($\mathrm{M_{BC}}$) defined as

$$\mathrm{M_{BC}} = \sqrt{E_{beam}^2 - \left(\sum_i p_i\right)^2},$$

where the p_i are the reconstructed momenta of the decay products of the B, and E_{beam} is the energy of the beam. The $\mathrm{M_{BC}}$ distribution has a resolution an order of magnitude better than the usual B invariant mass distribution. A fit to the $\mathrm{M_{BC}}$ distribution was used to count the number of Bs found.

The criteria used to select the B meson candidates varied with the decay mode used. Two quantities, however, were used in selecting all candidates: the B meson's polar angle θ_B and the difference between its reconstructed energy and the energy of the beam,

$$\Delta\mathrm{E} = E_{reconstructed} - E_{beam}.$$

The cut imposed on the polar angle was $|\cos(\theta_B)| \leq 0.95$, which takes advantage of the $\sin^2(\Theta_B)$ distribution resulting from angular momentum conservation in the decay of $\Upsilon(4S)$.

---

[1]Charge conjugate states are implied for all candidate particles

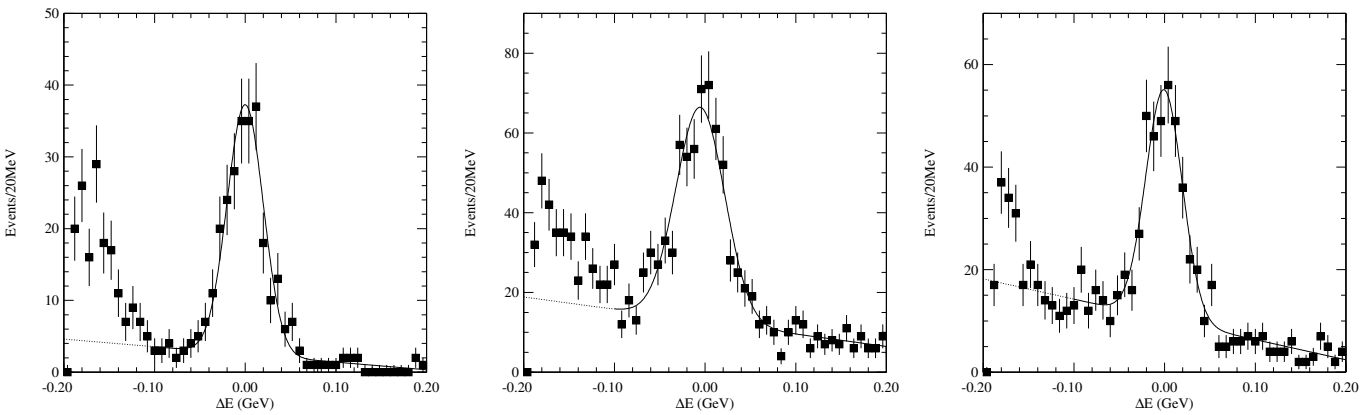

FIG. 1. The ΔE distributions of the $B^- \to D^0\pi^-$ modes. The figure on the left is the $D^0 \to K^-\pi^+$ mode, the center figure is the $D^0 \to K^-\pi^+\pi^0$ mode and the figure on the right is the $D^0 \to K^-\pi^+\pi^-\pi^+$ mode. The region below -100 MeV includes contributions from $B \to D(n\pi)$ where $n > 1$ and was exclude from the fit.

The ΔE distribution is centered on zero with a width ($\sigma_{\Delta \mathrm{E}}$) determined by the energy resolution of the individual particles in the final state. The ΔE widths were measured for each exclusive mode and were found to vary from 15 to 32 MeV. In Fig. 1 the on-4S ΔE distributions for the three $B^- \to D^0\pi^-$ modes are shown. The differences in energy resolutions are due to different number of charged tracks in the decay chain and, strongly, on the number of π^0 and their momentum. The enhancement in the region below -100 MeV is due primarily to $B^- \to D^0\rho^-$ decays where the π^0 from the ρ^- decay is missed and the decay is reconstructed as $B^- \to D^0\pi^-$.

A mode dependent ΔE cut of $2.5\sigma_{\Delta \mathrm{E}}$ was imposed on each candidate to discriminate against background events resulting from poorly reconstructed real B decays with a missing particle and/or from other B decays, that differ by one or more pion, and are miss-identified as the decay mode under investagation. Both of these backgrounds tend to populate the regions of ΔE away from 0.0. In B decays to a ρ^-, the resolution of ΔE is strongly dependent on the momentum of the π^0 from the ρ. Since the ρ is longitudinally polarized the dependence can be parameterized by the helicity angle Θ_h defined to be the angle between the direction of the π^0, in the ρ^- rest frame, and the direction of the ρ^- in the B candidate's rest frame. The cut on ΔE was varied as a function of Θ_h for these modes.

The large number of particles in each event can lead to multiple B candidates per event per mode that pass all the selection criteria. In these instances, the candidate with the "best" (*i.e.,* smallest) ΔE value was chosen. This procedure of picking the candidate with the best ΔE selects the correct candidate 86% of the time.

To reject continuum background we also cut on the cosine of the sphericity angle. The sphericity angle (Θ_f) is defined as the angle between the major sphericity axis calculated using all tracks consistent with a B candidate and the major sphericity axis calculated using the remaining tracks in the event. In continuum events, the topology of the event tends to be back-to-back and thus the sphericity angle populates the region near 0 or π. At the $\Upsilon(4S)$ $B\bar{B}$ pairs are produced nearly at rest and the decay topolgy is spherical. Thus for

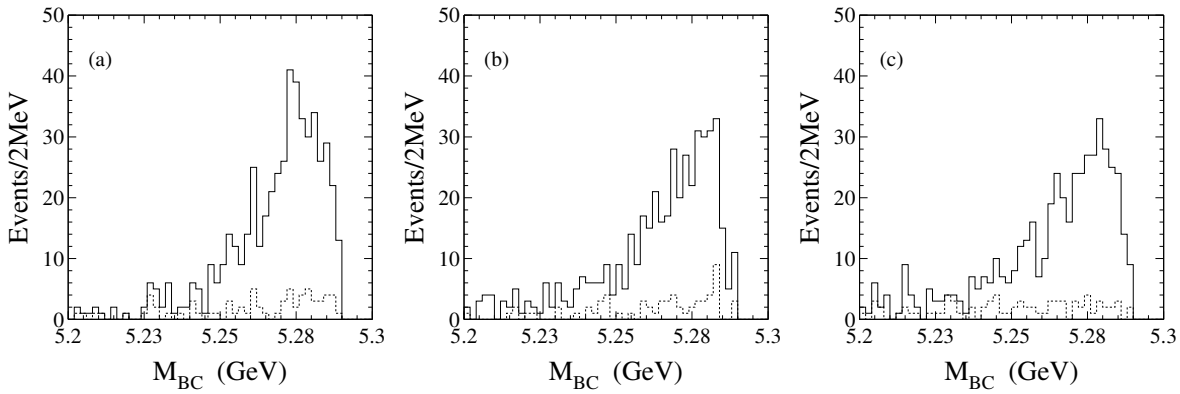

FIG. 2. The Background contribution from $D^{*0} \to D^0\gamma$ over the full ρ helicity range (solid histograms) and over half of the helicity range (dashed histograms). The figure on the left is the $D^0 \to K^-\pi^+$, the figure in the center is the $D^0 \to K^-\pi^+\pi^0$ and the figure on the right is the $D^0 \to K^-\pi^+\pi^-\pi^+$ D^0 sub-decay modes. The plots are M_{BC} distributions of $B^- \to D^{*0}\pi^-$ Monte Carlo events reconstructed as $B^- \to D^0\rho^-$.

$B\bar{B}$ events the sphericity angle can assume any value from 0 to 2π. To seperate $B\bar{B}$ events from continuum background we select events with $|\cos(\Theta_f)| < 0.7 - 0.9$.

V. $B \to D^{(*)}\pi$ MODES.

In B modes that decay to a charmed meson plus a single pion we used the cuts described in the preceding section with no additional requirements.

VI. $B \to D^{(*)}\rho$ MODES.

In $B \to D\rho$ modes, we employed a cut designed to take advantage of the spatial distribution of the rho-decay products. The spatial distribution is parameterized by the helicity angle (Θ_h) defined in Section IV. In B decays to a ρ plus a D^* we do not impose requirements on the helicity angle of either particle.

In the decay $B^- \to D^0\rho^-$ and in the $\bar{B}^0 \to D^+\rho^-$ channel we require $|\cos(\Theta_h)| \geq 0.4$. In the $B^- \to D^0\rho^-$ mode a substantial amount of background from $B^- \to D^{*0}\pi^-$ decays in which the D^{*0} decays to $D^0\gamma$ can be eliminated by discarding B candidates with a soft π^0 produced in the ρ^- decay. This decay can mimic a $B^- \to D^0\rho^-$ decay when a ρ^- is miss-reconstructed by combining the fast π^- from the B decay with a low momentum π^0 picked randomly from the large two shower combinatoric background [8]. This background can be removed by excluding the backward half – slow π^0 – region of the helicity angle. This additional requirement was imposed on all three $B^- \to D^0\rho^-$ modes and the branching fractions were recomputed as a consistency check. We found that the discrepancy between the branching fractions determined using the full and half helicity angle to be less than 1.2σ where σ is the statistical uncertainty.

TABLE I. D and D^* Branching Fractions

Decay Mode	Branching fraction (%)
$\mathcal{B}(D^{*0} \to D^0\pi^0)$	$63.6 \pm 2.3 \pm 3.3$ [10]
$\mathcal{B}(D^{*+} \to D^0\pi^+)$	$68.1 \pm 1.0 \pm 1.3$ [10]
$\mathcal{B}(D^0 \to K^+\pi^-)$	$3.91 \pm 0.08 \pm 0.17$ [11]
$\mathcal{B}(D^0 \to K^-\pi^+\pi^0)/\mathcal{B}(D^0 \to K^-\pi^+)$	$3.78 \pm 0.07 \pm 0.49$ [12]
$\mathcal{B}(D^0 \to K^-\pi^+\pi^-\pi^+)/\mathcal{B}(D^0 \to K^-\pi^+)$	2.05 ± 0.11 [13]
$\mathcal{B}(D^+ \to K^-\pi^+\pi^+)/\mathcal{B}(D^0 \to K^-\pi^+)$	$2.35 \pm 0.16 \pm 0.16$ [14]

VII. DETERMINATION OF BRANCHING FRACTIONS

The B branching fractions were determined by counting the numbers of events in each B decay corrected by the reconstruction efficiency (ϵ_{mc_b}), determined from Monte Carlo studies. In computing the branching fractions we also assume equal B^+ and B^0 production ($f_{+-}/f_{00} = 1.0$) at the $\Upsilon(4S)$ and, if available, we use CLEO II D and D^* branching fractions. Use of CLEO II D branching fraction measurements allows cancellation of common systematic errors some of which are anti-correlated with our measurements, thus reducing overall systematic errors. The D and D^* branching fractions and references used are listed in Table I.

The event yield for each decay mode was determined by fitting the continuum subtracted $\mathrm{M_{BC}}$ distribution for events that passed all the B meson requirements discussed in Sections II - IV. The continuum is scaled by the on to off $\Upsilon(4S)$ luminosity and corrected for the quadratic energy dependence of the continuum cross section. The distributions were then fit to a Gaussian of fixed width plus a background shape determined from Monte Carlo studies. The width of the Gaussian was fixed to a value determined from Monte Carlo for each decay mode separately.

In Fig. 3 the on-resonance $\mathrm{M_{BC}}$ distributions for the 12 B decay modes considered here are shown. In each plot, the fixed width Gaussian and the background function are superimposed on the $\mathrm{M_{BC}}$ distributions. In modes with a D^0 the three decay modes are combined.

The branching fraction for each mode is given in Tables II through IV. Three values were determined for each B decay mode that included a D^0 in the decay chain. The branching fraction averages, also listed in Tables II through IV, were computed by weighting all errors, statistical and systematic, taking into account the correlations of the systematic uncertainties among the different modes. Two systematic errors are quoted with each measurement; the first systematic error includes all contributions except the the D and D^* branching fraction errors. The combined systematic errors vary mode to mode are due to uncertainties in background systematics (less than 10%), tracking errors (2% /charged track, 5.0 % for slow charged tracks and 2.5% for showers), luminosity measurement (2.0%) and Monte Carlo statistics (less than 2.0%). The second systematic error includes only the contribution from the D and D^* measurement errors.

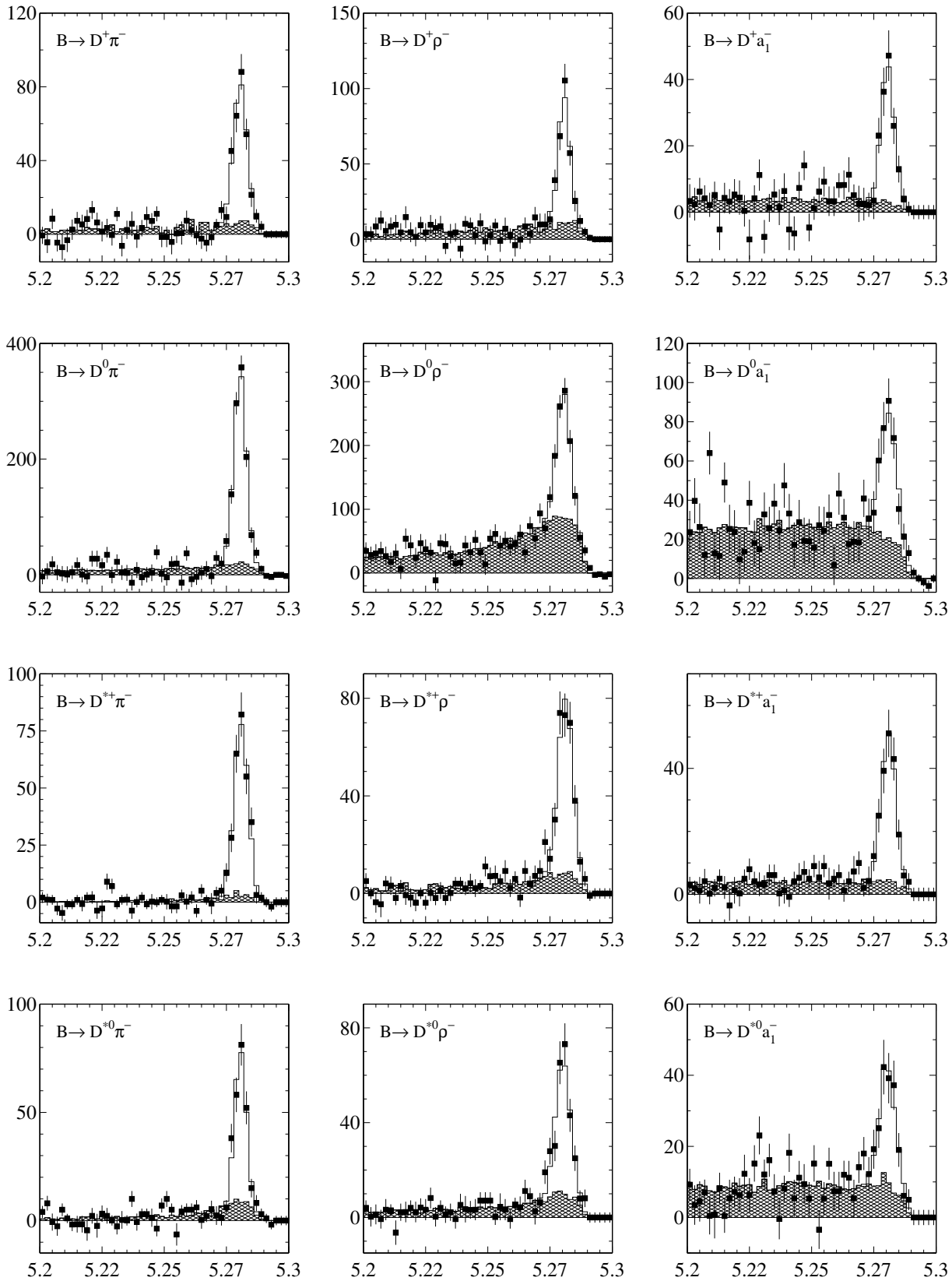

FIG. 3. The continuum-subtracted beam-constrained mass distributions for twelve B modes. In modes with a D^0, the three D^0 decay modes are combined. The hatched histograms shows the $B\bar{B}$ background spectrum, the open histograms is the sum of a Gaussian of fixed width plus a $B\bar{B}$ background distribution determined from Monte Carlo.

VIII. DETERMINATION OF BSW PARAMETERS

Determination of the magnitude and relative sign of the BSW parameters a_1 and a_2 allows for an estimate of the interference between internal and external spectator decay processes in charged B decays. To determine the parameters we use theoretical model predictions from Deandrea *et al.* (CDDFGN) [4], Neubert *et al.* (BSWII) [3]. These are used to relate the measured branching fractions to model predictions which are functions of a_1 and a_2. Both models rely on the factorization approximation and employ HQET to determine heavy-to-heavy form-factors. They differ primarily in how they estimate the heavy-to-light form-factors. To allow for model comparison we have re-scaled the decay constants f_ρ and f_D in the CDDFGN model to values used by BSWII. We also update the values of V_{cb} and the B lifetimes to current world averages. In addition, we use 1.0 for the B production fraction f_{+-}/f_{00}, consistent with the the value used to compute the branching fractions. The re-scaled theoretical relations are listed in Table V.

We determine the values of $|a_1|$, and a_2/a_1 in a least squares fitting procedure, using the averaged branching fractions and errors from Table II and III and the theoretical model predictions in Table V. The fit was carried out in two steps. First, the errors and correlations of the branching fractions were combined into a single measurement covariance matrix containing all the essential information. Then the measurements were fit to each of the two models using a generalized least squares method which used the full covariance matrix to weight the measurements.

The results are listed in Table VI and Table VII. We list the results, in Table VI, of the values of a_1 obtained by fitting to only the four B^0 branching fractions (3 degrees of freedom). In Table VII we list the results of the simultaneous fit for a_1 and a_2/a_1 using all eight B^0 and B^+ branching fractions (6 degrees of freedom). The two kinds of fits were done in order to check the consistency of the fits. Note that the simultaneous a_1, a_2/a_1 fit to the predictions of BSWII is significantly better than that to the CDDFGN model.

Two systematic errors are quoted for $|a_1|$ and a_2/a_1. They correspond to uncertainties from the experimental procedure and the D and/or D^* branching fraction as in the B branching fraction measurements. In Fig. 5 we show the variation of a_1 and a_2/a_1 as a function of the f_{+-}/f_{00} production ratio. We plot the dependence of the parameters on f_{+-}/f_{00} from 0.8 to 1.2 which corresponds to the current allowed range in the production fraction given the current measurement of the production-lifetime ratio and assuming equal B^-/B^0 lifetimes.

In Fig. 4 we plot the value of a_2/a_1 obtained for each ratio of branching fraction separately. The central values were taken from the average of the BSWII and CDDFGN model. To determine the value of a_2/a_1 from the ratios of $D^0a_1^-/D^+a_1^-$ and the $D^{*0}a_1^-/D^{*+}a_1^-$ we use the "New Model" (NSnew) results from Neubert-Stech [5]. The theoretical uncertainties are illustrated in Fig. 4 by the dark error bars which represent the spread in the value due to different theoretical inputs from the BSWII, CDDFGN and the (NSnew) models. The combined experimental errors are illustrated by the light error bars.

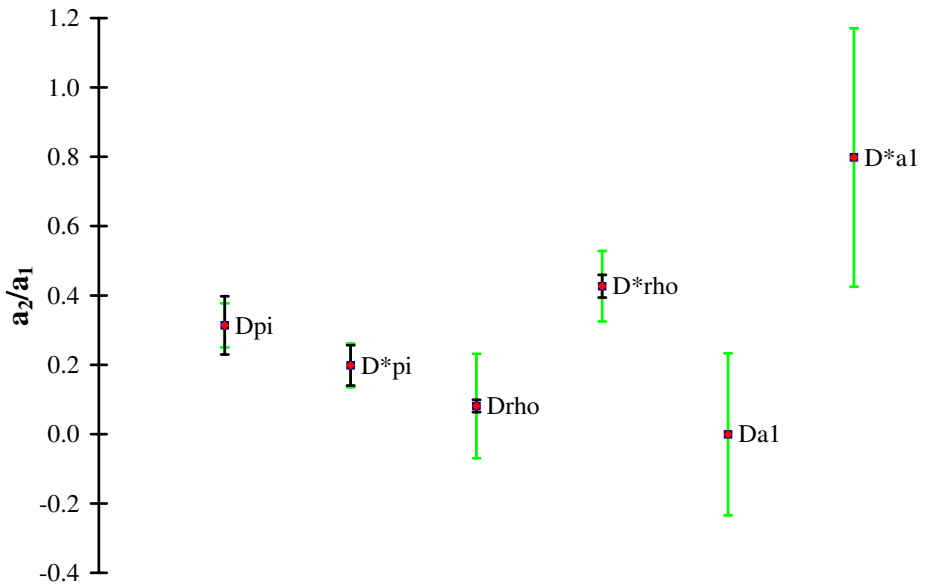

FIG. 4. The value of a_2/a_1 for each ratio used in the fit. The central values are the average of the CDDFGN and BSWII models. The light error bars show the combined experimental errors, the dark error bars show the spread due to the theoretical model predictions including the "New Model" from Neubert-Stech.

IX. CONCLUSION

We have presented new results on twelve hadronic decays of the B^0 and B^- mesons using the entire CLEO II data sample, increasing the data sample by a factor 3 over the previously published CLEO II results. Two modes, the $B^- \to D^0 a_1^-$ and $\bar{B}^0 \to D^+ a_1^-$ are presented with errors below 50% for the first time. The branching fraction measurements were used to determine the BSW parameters a_1 and a_2, confirming a positive value for the relative sign of a_1 and a_2.

X. ACKNOWLEDGEMENTS

We gratefully acknowledge the effort of the CESR staff in providing us with excellent luminosity and running conditions. J.P.A., J.R.P., and I.P.J.S. thank the NYI program of the NSF, M.S. thanks the PFF program of the NSF, G.E. thanks the Heisenberg Foundation, K.K.G., M.S., H.N.N., T.S., and H.Y. thank the OJI program of DOE, J.R.P., K.H., M.S. and V.S. thank the A.P. Sloan Foundation, R.W. thanks the Alexander von Humboldt Stiftung, and M.S. thanks Research Corporation for support. This work was supported by the National Science Foundation, the U.S. Department of Energy, and the Natural Sciences and Engineering Research Council of Canada.

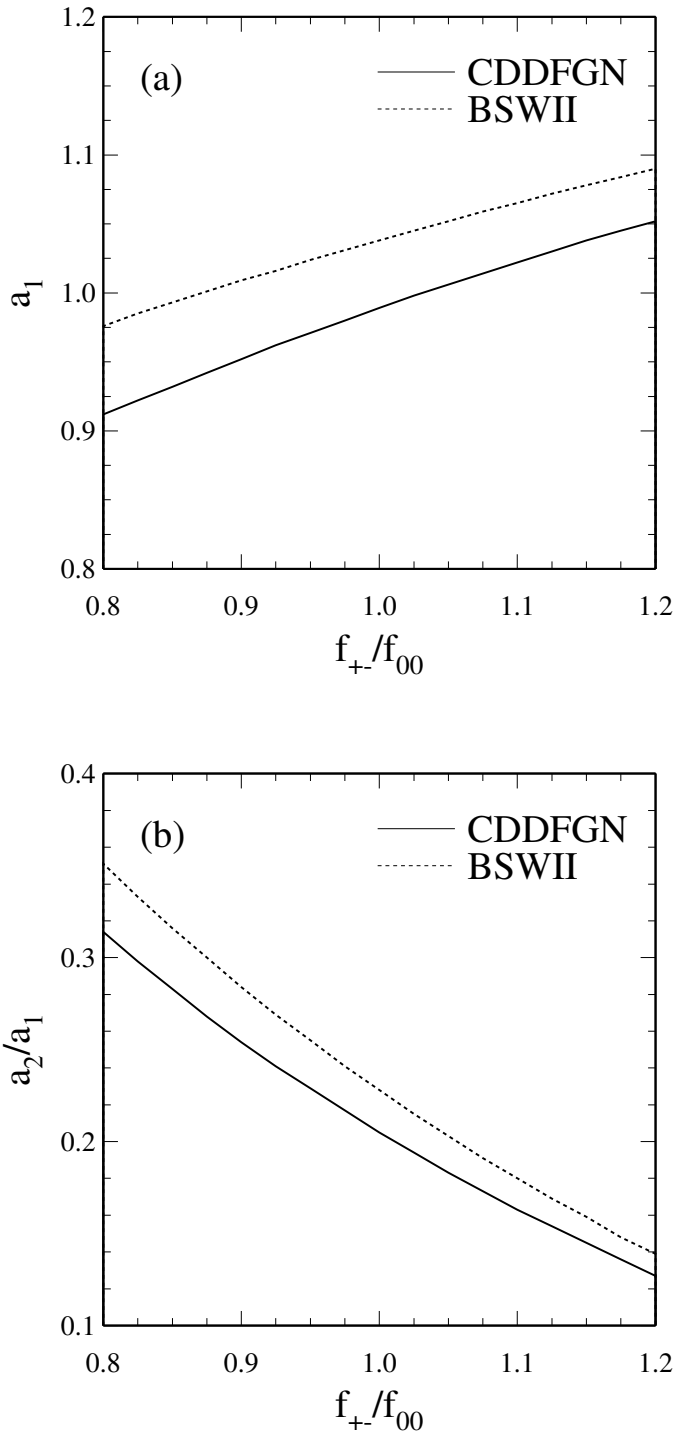

FIG. 5. The dependence of the BSW parameters on the f_{+-}/f_{00} production fraction in (a) the dependence of $|a_1|$, and (b) the dependence of a_2/a_1.

TABLE II. Table of branching fractions $B \to D^{(*)}\pi^-$ decays

B Mode	D Mode	Yield	$\epsilon_{mc}(\%)$	$\mathcal{B}(\%)$	$\mathcal{B}(\%)$ average
$D^+\pi^-$	$K^-\pi^+\pi^+$	240	31.7	0.250 ± 0.022	$0.250 \pm 0.022 \pm 0.024 \pm 0.024$
	$K^-\pi^+$	65	33.3	0.222 ± 0.040	
$D^{*+}\pi^-$	$K^-\pi^+\pi^0$	116	14.8	0.235 ± 0.029	$0.234 \pm 0.021 \pm 0.022 \pm 0.010$
	$K^-\pi^+\pi^-\pi^+$	67	14.8	0.252 ± 0.040	
	$K^-\pi^+$	239	40.8	0.455 ± 0.034	
$D^0\pi^-$	$K^-\pi^+\pi^0$	479	19.1	0.510 ± 0.037	$0.473 \pm 0.025 \pm 0.033 \pm 0.014$
	$K^-\pi^+\pi^-\pi^+$	296	21.5	0.523 ± 0.041	
	$K^-\pi^+$	43	15.3	0.342 ± 0.073	
$D^{*0}\pi^-$	$K^-\pi^+\pi^0$	93	7.4	0.406 ± 0.067	$0.392 \pm 0.046 \pm 0.033 \pm 0.028$
	$K^-\pi^+\pi^-\pi^+$	71	7.7	0.547 ± 0.100	

TABLE III. Table of branching fractions $B \to D^{(*)}\rho^-$ decays [16]

B Mode	D Mode	Yield	$\epsilon_{mc}(\%)$	$\mathcal{B}(\%)$	$\mathcal{B}(\%)$ average
$D^+\rho^-$	$K^-\pi^+\pi^+$	251	10.5	0.789 ± 0.069	$0.789 \pm 0.069 \pm 0.093 \pm 0.077$
	$K^-\pi^+$	77	10.8	0.805 ± 0.107	
$D^{*+}\rho^-$	$K^-\pi^+\pi^0$	110	4.9	0.666 ± 0.086	$0.734 \pm 0.061 \pm 0.074 \pm 0.030$
	$K^-\pi^+\pi^-\pi^+$	63	4.6	0.749 ± 0.136	
	$K^-\pi^+$	145	14.2	0.794 ± 0.112	
$D^0\rho^-$	$K^-\pi^+\pi^0$	364	6.7	1.110 ± 0.116	$0.920 \pm 0.080 \pm 0.072 \pm 0.028$
	$K^-\pi^+\pi^-\pi^+$	235	7.1	1.256 ± 0.150	
	$K^-\pi^+$	62	5.4	1.406 ± 0.211	
$D^{*0}\rho^-$	$K^-\pi^+\pi^0$	111	2.5	1.418 ± 0.186	$1.277 \pm 0.129 \pm 0.113 \pm 0.090$
	$K^-\pi^+\pi^-\pi^+$	44	2.6	1.021 ± 0.242	

TABLE IV. Table of branching fractions $B \to D^{(*)}a_1^-$ decays [17]

B Mode	D Mode	Yield	$\epsilon_{mc}(\%)$	$\mathcal{B}(\%)$	$\mathcal{B}(\%)$ average
$D^+a_1^-$	$K^-\pi^+\pi^+$	136	8.6	0.834 ± 0.088	$0.834 \pm 0.088 \pm 0.115 \pm 0.081$
	$K^-\pi^+$	49	8.5	1.333 ± 0.235	
$D^{*+}a_1^-$	$K^-\pi^+\pi^0$	66	4.0	1.006 ± 0.160	$1.157 \pm 0.120 \pm 0.155 \pm 0.049$
	$K^-\pi^+\pi^-\pi^+$	45	3.7	1.348 ± 0.266	
	$K^-\pi^+$	58	10.9	0.785 ± 0.155	
$D^0a_1^-$	$K^-\pi^+\pi^0$	98	3.8	0.986 ± 0.163	$0.887 \pm 0.104 \pm 0.107 \pm 0.028$
	$K^-\pi^+\pi^-\pi^+$	86	5.7	1.090 ± 0.209	
	$K^-\pi^+$	29	4.1	1.733 ± 0.476	
$D^{*0}a_1^-$	$K^-\pi^+\pi^0$	56	2.1	1.781 ± 0.376	$1.597 \pm 0.250 \pm 0.209 \pm 0.115$
	$K^-\pi^+\pi^-\pi^+$	24	2.2	1.333 ± 0.438	

TABLE V. Branching Fractions Model Predictions

B mode	$\mathcal{B}$ BSWII	$\mathcal{B}$ CDDFGN
$D^+\pi^-$	$0.25a_1^2$	$0.26a_1^2$
$D^{*+}\pi^-$	$0.24a_1^2$	$0.26a_1^2$
$D^+\rho^-$	$0.59a_1^2$	$0.58a_1^2$
$D^{*+}\rho^-$	$0.67a_1^2$	$0.77a_1^2$
$D^0\pi^-$	$0.25(a_1+1.2a_2)^2$	$0.26(a_1+1.2a_2)^2$
$D^{*0}\pi^-$	$0.24(a_1+1.3a_2)^2$	$0.26(a_1+1.7a_2)^2$
$D^0\rho^-$	$0.63(a_1+0.66a_2)^2$	$0.58(a_1+0.5a_2)^2$
$D^{*0}\rho^-$	$0.67(a_1^2+0.64a_2^2+1.5a_1a_2)$	$0.77(a_1^2+0.69a_2^2+1.4a_1a_2)$

TABLE VI. Results of Fit to BSW Parameter a_1

	$\lvert a_1\rvert$	χ^2/dof
CDDFGN	$0.984 \pm 0.027 \pm 0.042 \pm 0.020$	4.8/3
BSWII	$0.997 \pm 0.028 \pm 0.044 \pm 0.022$	3.8/3

TABLE VII. Results of Fit to BSW Parameters a_1 and a_2

	$\lvert a_1\rvert$	a_2/a_1	χ^2/dof
CDDFGN	$0.953 \pm 0.026 \pm 0.042 \pm 0.020$	$0.232 \pm 0.037 \pm 0.022 \pm 0.018$	20.3/6
BSWII	$0.989 \pm 0.028 \pm 0.043 \pm 0.021$	$0.264 \pm 0.039 \pm 0.025 \pm 0.019$	9.1/6

REFERENCES

[1] M. Bauer, B. Stech and M. Wirbel, Z. Phys. **C29**, 639 (1985).

[2] M.J. Dugan, B. Grinstein, Phys. Lett. , B225 583 (1990).

[3] M. Neubert, V. Rieckert, B. Stech and Q. P. Xu in *Heavy Flavours* edited by A. J. Buras and H. Lindner, World Scientific, Singapore (1992).

[4] A. Deandrea, N. Di Bartolomeo, R. Gatto and G. Nardulli, Phys. Lett. B 318, 549 (1993).

[5] M. Neubert, B. Stech, preprint hep-ph/9705292, to appear in: the Second Edition of Heavy Flavours, edited by A.J. Buras and M. Linder (World Scientific, Singapore)

[6] CLEO collaboration, Y. Kubota *et al.* , Nucl. Instr. and Meth. **A320**, 66 (1992). For a complete description of the CLEO II detector

[7] CLEO Collaboration, M. S. Alam *et al.* , Phys. Rev. D **50**, 43 (1994).

[8] J. L. Rodriguez, University of Florida Dissertation (1995).

[9] G. Fox and S. Wolfram, Phys. Rev. D , 41 1581 (1978).

[10] CLEO Collaboration, F. Butler *et al.* , Phys. Rev. Lett. **69**, 2041 (1992).

[11] CLEO Collaboration, D. Akerib *et al.* , Phys. Rev. Lett. **71**, 3070 (1993). The value quoted for the absolute branching fraction is the value without radiative corrections.

[12] CLEO Collaboration, B. Barish *et al.* , Phys. Lett. **B373**, 334 (1996)

[13] Particle Data Group, M. Aguilar-Benitez *et al.* , Phys. Rev. D **50**, 1173 (1994).

[14] CLEO Collaboration, R. Balest *et al.* , Phys. Rev. Lett. **72**, 2328 (1994).

[15] CLEO Collaboration, B. Barish *et al.* , Phys. Rev. D **51**, 1014 (1995).

[16] The non-resonant $\pi^0\pi^-$ component in $D^{(*)}\rho^-$ is small. It ranges from less than 2.5% to 9.0% depending on the mode. For these modes we neglect non-resonant contributions. This analysis was performed in reference [7] on approximately 1/3 of the current data sample.

[17] The non-resonant $\pi\pi\pi$ and $\pi\rho^0$ component in $D^{(*)}a_1^-$ was found to be less than 12% and 24% in D^0a_1 and D^+a_1 decays at the 90% Confidence Level [8]. The event yields were corrected accordingly for the $D^{(+,0)}a_1^-$ modes. In D^*a_1 the contributions from non-resonant $\pi^-\rho^0$ and $D^{**}\rho$ were found to be less 9.4% and 10.6% respectively at the 90% confidence level [7]. We thus neglect non-resonant contributions to both $D^{(+,0)}a_1^-$ modes.